Composite Lattice Pattern Formation in a Wide-Aperture Thin-Slice Solid-State Laser with Imperfect Reflective Ends

Kenju Otsuka,* Yoshihiko Miyasaka, and Tatsuro Narita
Department of Human and Information Science, Tokai University, 1117 Kitakaname, Hiratsuka, Kanagawa 259-1292, Japan

Shu-Chun Chu†
Department of Photonics, Institute of Electro-Optical Engineering, National Chiao-Tung University, Ta Hsueh Rd., Hsinchu City 300, Taiwan

Chi-Ching Lin and Jing-Yuan Ko
Department of Physics, National Kaohsiung Normal University, 116 Ho-Ping First Rd., Kaohsiung 802, Taiwan
(Received 20 March 2006; published 20 November 2006)

We observed self-formations of multiple lasing channels and two-dimensional lasing patterns consisting of composite local modes having different lasing frequencies in a laser-diode-pumped wide-aperture thin-slice solid-state laser with imperfect reflective end surfaces. Global patterns resembling higher-order Hermite-Gaussian modes or possessing N-fold rotational symmetries were experimentally shown to appear due to the standard polished surface roughness of closely spaced reflective ends and nonlinear modal interactions.

DOI: 10.1103/PhysRevLett.97.213901 PACS numbers: 42.65.Sf, 42.65.Tg, 89.75.Kd

Pattern formation in spatially extended nonequilibrium systems has attracted much attention in nonlinear dynamics. The so-called transverse effect has appeared as spontaneous pattern formations in nonlinear optics and lasers which featured rolls, hexagons, vortices, and a variety of solitons created by various nonlinearities [1]. Various cavity solitons and nonlinear patterns in optics have been investigated in wide-aperture lasers including vertical-cavity semiconductor lasers [2–4]. On the other hand, the effect of surface irregularities on nonlinear pattern formations in vertical-cavity microresonators has also been reported [4,5]. Here, we report lasing patterns resulting from the formation of "lasing channels" (hereafter called local modes) in a laser-diode-pumped wide-aperture thin-slice solid-state laser with imperfect reflective ends. The observed lasing patterns, whose global mode patterns resemble higher-order Hermite-Gaussian modes and nonlinear patterns possessing rotational symmetries, were found to be formed by self-induced decomposition into multiple local modes having different optical frequencies and intensities. Observed composite local-mode complexes are experimentally shown to result from a statistical surface roughness of the closely spaced reflective ends, which have a standard polished surface flatness.

The experimental setup is shown in Fig. 1. A 5-mm-square 3 at. %-doped a-cut Nd:$GdVO_4$ laser (CRYSTECH) with a 0.3-mm-thick plane-parallel Fabry-Perot resonator configuration was attached to a Cu heat sink that had a 3-mm-diameter hole in the center. The polished surface flatness was $\lambda/8$ at the He-Ne laser wavelength of 632.8 nm (i.e., 79 nm), where the surface quality of the polished crystal was 10/5 scratch/dig per MIL-O-13830. One end-surface was coated to be transmissive at the laser-diode (LD) pump wavelength of 808 nm (85% transmission) and highly reflective (99.9%) at the lasing wavelength of 1063 nm. The other surface was coated to be 2% transmissive at 1063 nm. We collimated the LD pump beam and passed it through an anamorphic prism pair to transform the elliptical beam into a circular one. Then, the circular beam was focused on the laser crystal surface by an aspherical lens with a focal length of 5 cm, where the focused beam diameter was measured to be 710 μm. The threshold pump power was 300 mW and the slope efficiency was 10%. Because of crystal anisotropy, the lasing light was π polarized along the c axis (primary optic axis) of the Nd:$GdVO_4$ crystal, as depicted in Fig. 1.

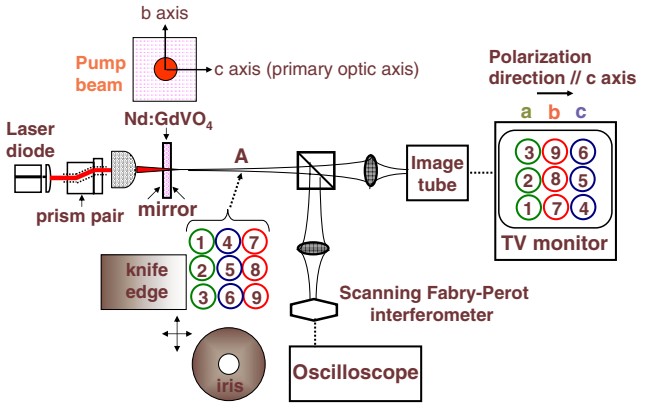

FIG. 1 (color online). Experimental configuration of a thin-slice Nd:$GdVO_4$ laser with laser-diode pumping. The lasing beam from individual spots on the crystal surface are crossing as depicted by mode numbers for the composite lattice patterns [3 × 3] in Fig. 2(c).

Global oscillation spectra measured using a multiwavelength meter with a resolution of 0.1 nm showed a single longitudinal-mode operation. Here, the gain bandwidth of Nd:$GdVO_4$ was 3 nm while the longitudinal-mode spacing was 0.94 nm. Lasing spatial patterns changed depending on the pump beam diameter, pump position (i.e., local surface undulation structure of the reflective ends within the lasing beam spot), and a slight tilt of the crystal (i.e., lasing direction) against the pump direction, i.e., mode matching conditions between the pump and lasing beam profiles. Lasing patterns were measured with a PbS infrared image tube placed 20 cm away from the laser after the beam diameter was decreased with a lens such that the focused beam diameter did not exceed the detector area, as depicted in Fig. 1. Detailed optical spectra were measured with a scanning Fabry-Perot interferometer with a frequency resolution of 6.6 MHz.

Examples of pump-dependent far-field transverse patterns and detailed optical spectra corresponding to patterns are shown in Fig. 2 for a constant pump position. Because of the surface roughness of the reflective ends of an extremely short Fabry-Perot optical cavity, perfect Hermite-Gaussian transverse modes could not be formed. Starting from a lasing pattern consisting of three bright spots in the upper row, an irregular transverse pattern consisting of local modes with different frequencies was formed as shown in Fig. 2(a) with increasing pump power, i.e., transverse active area. The observed frequency separations of local modes are thought to be determined by the roughness on the scale of the pump beam diameter rather than by the averaged roughness across the whole crystal. With increasing pump power, the thermal lens effect, which results from the gradient refractive index and cavity length changes, increased together with the active area, and we consider that the lasing channels changed. Note that lasing beams from localized cavity modes with small divergences were found to be emitted not in parallel, but with slightly oblique angles from the laser. No qualitative differences were identified between near-field and far-field (i.e., diffraction) patterns presumably because oblique beams were unable to interfere in the far fields that we measured. The resultant beam crossing is depicted by mode numbers in Fig. 1.

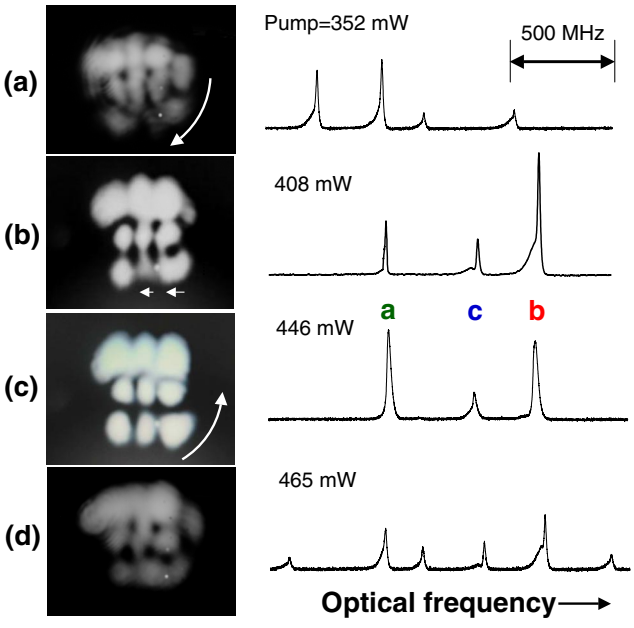

FIG. 2 (color online). Far-field patterns and corresponding optical power spectra indicating the formation of a [3 × 3] composite lattice pattern with increasing the pump power.

As the pump power was further increased, 9-spot lasing patterns [Figs. 2(b) and 2(c)] resembling the Hermite-Gaussian TEM_{22} mode appeared. It is interesting to note that the 9-spot pattern (b) was formed by fusion accompanied by a clockwise rotation of local spots in (a) as shown by the arrow, where the optical power spectrum was clustered into three groups, in which each of mode groups b and c consists of two closely spaced frequency components. When the pump power was slightly increased, the frequency locking occurred in each group of mode groups in the optical spectrum of Fig. 2(b), where spots in the bottom rows shifted simultaneously as indicated by arrows. Consequently, the clear [3 × 3] pattern was formed as shown in Fig. 2(c). As the pump power was increased, pattern (c) was deformed into pattern (d), which featured fission accompanied by a counterclockwise segregation of spots in pattern (c).

Let us identify the 9-spot transverse lasing pattern, i.e. [3 × 3] array, shown in Fig. 2(c), by examining detailed optical spectra of individual spots and phase relationships among the spots. Figure 3(a) shows selected spot(s) in the top row of the pattern in Fig. 2(c) and corresponding

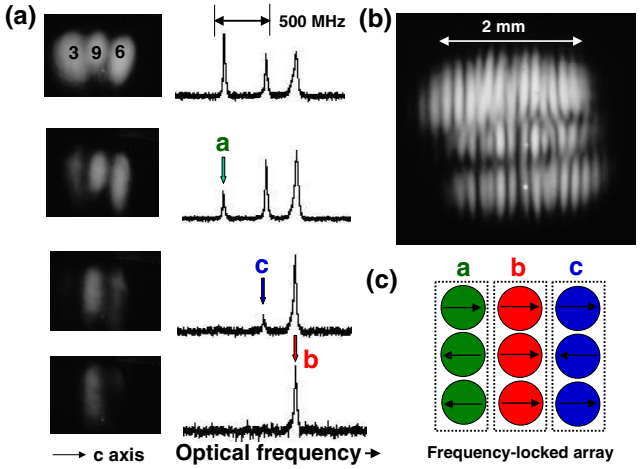

FIG. 3 (color online). (a) Selected far-field spot(s) and corresponding optical power spectra in the [3 × 3] composite lattice pattern shown in Fig. 2(c). (b) Interferogram. (c) Phase relationship of lasing fields within the frequency-locked modes, where field phases are depicted by arrows.

optical spectra, where each lasing spot was selected by adjusting a knife edge or an iris (i.e., pin hole) with variable apertures at position A in Fig. 1. The lasing frequencies of all the spots were similarly identified. We found that lasing spots in each column oscillated at exactly the same frequency. In other words, three localized modes in each column were locked to the same frequency, where lasing frequencies were different for different frequency-locked groups. To be more specific, just before the frequency locking occurred, the frequencies of modes in the bottom rows of arrays in Fig. 2(b) were slightly different from those of the other two modes in the same arrays as shown in the optical spectrum of Fig. 2(b). In short, three bright spots (strong modes) in the initial pattern were found to oscillate at their own frequencies in a transition process to the clustering, and other local modes in the same column were frequency locked to the strong mode successively through nearest-neighbor field couplings. The stable locking state was maintained in the pump-power region of 415 mW $\leq P \leq$ 455 mW.

Such a clustering into different frequency-locked mode groups can be understood in the framework of Kuramoto's model of general coupled nonlinear oscillators in a variety of physical systems [6]. In lasers, field coupling (i.e., spatial overlapping) among localized modes is attributed to synchronization phenomena [7]. To identify phase relationships among localized modes in each group, we observed an interferogram by replacing the beam splitter and the scanning Fabry-Perot interferometer in Fig. 1 by a 1-mm-thick glass plate and the PbS image tube, respectively. The observed interferogram pattern corresponding to the 9-spot pattern is shown in Fig. 3(b). The phase relationships among spots estimated from fringe flows [Fig. 3(b)] are depicted in Fig. 3(c). Modes in the central column are almost in phase, exhibiting straight fringe flows, while modes in the outer columns show different phase relationships, in which 3 spots in each column were frequency locked in this case. It is obvious that the phase relationships among the 9 spots were completely different from those of the TEM_{22} mode. The self-organized clustering into frequency-locked arrays was found to occur for arrays whose directions were perpendicular to the primary optic axis (i.e., polarization direction) of the Nd:$GdVO_4$ crystal (tetragonal system; $I4_1/amd$ space group) as shown in Fig. 1. In other words, the frequency-locked composite lattice was formed when the pump position was tuned such that the bright spots having different frequencies appeared in the primary optic axis (i.e., polarization direction) near the threshold pump power. Otherwise, irregular patterns consisting of local modes appeared. A clear understanding of observed behavior has yet to be known, however, our observation suggests that the anisotropic property of Nd:$GdVO_4$ crystal affects the pattern formation.

By changing the pump position and diameter, we could produce a variety of local-mode complexes with increasing pump power, depending on the initial lasing pattern. Examples of near-field patterns and corresponding optical spectra are shown in Fig. 4, where (a) TEM_{11}, (b) TEM_{32}, and (c) TEM_{33} resemblances, consisting of different frequency-locked local-mode groups, were formed. These resemblances were found to be formed when the pump position was adjusted such that initial lasing patterns started from either 2 or 4 bright spots along the primary optic axis (i.e., polarization direction) in the far-field patterns in Figs. 4(a)–4(c) similar to Fig. 3. As the pump power was increased, the global field-intensity profile approached the Hermite-Gaussian mode (ground state), i.e., the global minimum of the transverse eigenmodes in the unperturbed Fabry-Perot cavity, accompanied by the clustering into different frequency-locked local-mode groups. Here, the frequency-locking state in each column shown in Figs. 4(a)–4(c) is considered to be governed by strong localized modes (bright spots) having their own frequencies, which led to successive modal frequency locking in the column directions.

In order to identify the dominant contribution of surface inhomogeneities to the formation of localized lasing channels, we replaced the Nd:$GdVO_4$ laser by a 0.3-mm-thick $LiNdP_4O_{12}$ (LNP) laser having the same surface flatness and thermal coefficients for the lens effect [8]. In this case, the increased optical confinement due to the thermal lens effect overwhelmed the effect of surface roughness because of the smaller thermal conductivity of LNP [8]

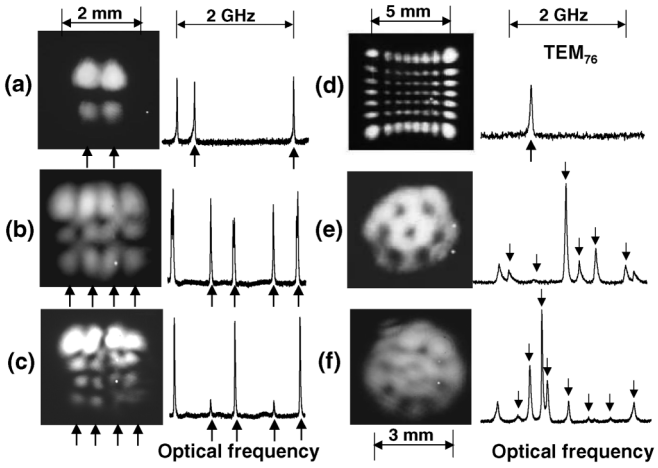

FIG. 4. (a)–(c) Far-field patterns and corresponding optical power spectra for composite $[m \times n]$ lattices: (a) $P = 390$ mW (stable frequency-locking region: 380 mW $\leq P \leq$ 415 mW), (b) $P = 410$ mW (400 mW $\leq P \leq$ 430 mW), (c) $P = 435$ mW (430 mW $\leq P \leq$ 440 mW). (d) single-frequency TEM_{76} mode observed in the LNP laser oscillating at $\lambda = 1060$ nm, $P =$ 435 mW. (e),(f) Far-field patterns and corresponding power spectra for composite lattices with sixfold and eightfold rotational symmetries: (e) $P = 505$ mW (stable region: 430 mW $\leq$ $P \leq$ 510 mW). (f) $P = 466$ mW (440 mW $\leq P \leq$ 500 mW). Scales of observed far-field patterns are the same for (a)–(c) [2 mm] and (e)–(f) [3 mm], respectively.

(i.e., 1/4 that of Nd:$GdVO_4$), and orthogonal Hermite-Gaussian modes were formed without forming lasing channels. An example of the result obtained under the same pumping condition as Fig. 4(c) is shown in Fig. 4(d). Here, reflecting the excellent match between pump and lasing modes, a single-frequency TEM_{76} mode oscillation was obtained. On the other hand, when the LD pump beam was tightly focused by a microscope objective lens to a diameter of 100 μm, the 0.3-mm-thick Nd:$GdVO_4$ showed a transverse-mode transition from an irregular to a Gaussian (i.e., TEM_{00} mode) lasing pattern with increasing pump power [8] due to increased heat generation (i.e., thermal lens effect) due to the tightly focused pump beam as compared with the 710-μm-diameter pumping.

As the pump beam diameter was increased by shifting the laser position from the focal plane, transverse patterns possessing N-fold rotational symmetries appeared with increasing pump power. From the observed optical spectra, it is obvious that these patterns were formed by local cavity modes having different lasing frequencies and intensities. Localized cavity modes were also found to be emitted not in parallel but with slightly oblique angles from the laser similar to $[m \times n]$ composite lattice patterns. Here, the frequency locking among local modes was not established, unlike in the case of Hermite-Gaussian resemblances, because of the absence of simple nearest-neighbor field couplings. Although these lasing patterns possess curious rotational symmetries, the observed composite local-mode lattices are totally different from such nonlinear patterns as honeycomb and Akhseals patterns, which arise through the interaction of multiple plane waves in a nonlinear resonator containing a quadratic or a Kerr-type nonlinearity [9,10]. See Ref. [11] for supplementary material showing formations of $[m \times n]$ lattice patterns and N-fold rotational symmetric patterns.

Beating-type complicated high-speed intensity modulations at the beat frequencies of local modes, which are 2 orders of magnitude higher than the relaxation oscillation frequency, appeared when frequency locking failed for all the composite lattice lasing patterns [12].

In conclusion, the self-formation of multiple lasing channels and associated curious lattice patterns, which consist of different local modes, featuring $[m \times n]$ or N-fold rotational symmetries, has been demonstrated in an LD-pumped wide-aperture thin-slice solid-state laser. The localization and coupling of lasing cavity fields by rough reflective end surfaces within the lasing beam area have been clarified to be the key mechanism of self-induced organization into composite local-mode lattices. The localized-mode complexes that we observed should provide some insight into optical localization and self-induced dissipative pattern formation in wide-aperture thin-slice cavity lasers through small irregularities in standard polished reflective ends. Because of the statistical nature of the surface irregularity, various lasing patterns, besides those mentioned here, are expected to be formed depending on the pumping conditions. A theoretical study of the observed formation of local lasing modes and reorganization into composite lattice patterns is now in progress.

*Electronic address: ootsuka@keyaki.cc.tokai-u.ac.jp
†Permanent address: Department of Physics, National Cheng Kung University, No.1, University Road, Tainan City 701, Taiwan.

[1] F. T. Arecchi, S. Boccaletti, and P. Ramazza, Phys. Rep. **318**, 1 (1999); W. J. Firth, in *Self-Organization in Optical Systems and Applications in Information Technology*, edited by M. A. Vorontsov and W. B. Miller (Springer-Verlag, Berlin 1995), p. 69; L. A. Lugiato, M. Brambilla, and A. Gatti, in *Advances in Atomic, Molecular and Optical Physics*, edited by B. Bederson and H. Walther (Academic, New York, 1998), Vol. 40, p. 229.
[2] N. N. Rosanov, *Spatial Hysteresis and Optical Patterns* (Springer, New York, 2002); N. N. Rosanov, S. V. Fedorov, and A. N. Shatsev, Phys. Rev. Lett. **95**, 053903 (2005).
[3] W. J. Firth and G. K. Harkenss, in Springer Series in Optical Sciences, edited by S. Trillo and W. Torruellas (Springer-Verlag, Berlin, 2001), Vol. 82, p. 343; L. A. Lugiato, IEEE J. Quantum Electron. **39**, 193 (2003).
[4] T. Ackemann *et al.*, Opt. Lett. **25**, 814 (2000).
[5] X. Tang *et al.*, IEEE J. Quantum Electron. **33**, 927 (1997); R. Kuszelewicz *et al.*, Phys. Rev. Lett. **84**, 6006 (2000).
[6] Y. Kuramoto, in *Chemical Oscillations, Waves, and Turbulence*, edited by H. Haken (Springer-Verlag, Berlin, 1984).
[7] R. Roy and K. S. Thornburg, Jr., Phys. Rev. Lett. **72**, 2009 (1994); K. Otsuka *et al.*, Phys. Rev. Lett. **84**, 3049 (2000); K. Otsuka, *Nonlinear Dynamics in Optical Complex Systems* (Springer, New York, 2000).
[8] Y. Miyasaka *et al.*, Opt. Express **13**, 7928 (2005).
[9] S. Barland *et al.*, Europhysics News **34**, 136 (2003).
[10] M. A. Vorontsov, Quantum Electron. **23**, 269 (1993); M. A. Vorontsov *et al.*, Chaos Solitons Fractals **4**, 1701 (1994).
[11] See EPAPS Document No. E-PRLTAO-97-038648 for supplementary videos that show pump-dependent pattern changes indicating the formation of TEM_{11}, TEM_{22} resemblances with increasing the pump power, and sixfold, eightfold rotational symmetric patterns with first increasing and then decreasing pump power. For more information, see http://www.aip.org/pubservs/epaps.html.
[12] C.-Z. Ning, Opt. Lett. **27**, 912 (2002).